ELSEVIER

Biophysical Chemistry 96 (2002) 53–76

Biophysical Chemistry

www.elsevier.com/locate/bpc

Interactions of the DNA intercalator acridine orange, with itself, with caffeine, and with double stranded DNA

Mark B. Lyles, Ivan L. Cameron*

Department of Cellular and Structural Biology, University of Texas Health Science Center at San Antonio, 7703 Floyd Curl Drive, San Antonio, TX 78229-3900, USA

Received 30 July 2001; received in revised form 10 January 2002; accepted 30 January 2002

Abstract

Caffeine (CAF) inhibits the intercalation of acridine orange (AO) into cellular DNA. Optical absorption and fluorescence spectroscopy were employed to determine the molecular interactions of AO with itself, with CAF, and with double stranded herring sperm DNA (dsDNA). AO dimerization was observed at concentrations >2 μmol. The sharp increase in fluorescence (λ_{em} = 530 nm) at 5 μmol of AO was attributed to AO multimer formation. From 0.5 to 5.0 μmol, the AO self-association binding constant (K_{assoc}) was determined to be 38 620 mol^{-1}, however, the presence of 150 mmol NaCl increased K_{assoc} to 118 000 mol^{-1} attributed to the charge neutralization. The K_{assoc} for AO with CAF was confirmed to be 256 mol^{-1}. K_{assoc} for the binding of AO with 20 μmol DNA ranged from, 32 000 mol^{-1} at 2 μmol AO, to approximately 3700 mol^{-1} at 10 μmol AO, in the absence of NaCl. This AO concentration dependency of K_{assoc} value with DNA was attributed to AO intercalation into dsDNA at high dsDNA/AO ratios, and electrostatic binding of AO to dsDNA at low AO ratios. The findings provide information used to explain fluorescence intensity values at λ_{em} at 530 nm from studies that combine AO, caffeine, and dsDNA. © 2002 Elsevier Science B.V. All rights reserved.

Keywords: Xanthines; Acridine orange; Caffeine; Competitive interactions; Desmutagens; Intercalators

1. Introduction

DNA intercalating agents disrupt the normal function of cellular DNA and can lead to interference with gene expression, gene transcription, mutagenesis, carcinogenesis, and cell death [1,2]. Many carcinogenic chemicals damage DNA [1–3]. Several strategies for the chemoprevention of cancer aim to block this initial DNA damage, either by altering the metabolic pathways away from activation and/or towards detoxification, or by 'scavenging' the reactive electrophiles [4–6]. Antimutagenic agents that trap mutagens have been termed 'interceptor molecules' or 'desmutagens', and may represent an important first line of defense against mutagens and carcinogens [6–8].

Several laboratories have reported on the interaction of xanthines and xanthine analogs with carcinogenic polyaromatic DNA intercalators

*Corresponding author. Tel.: +1-210-567-3896; fax: +1-210-567-3803.

E-mail address: cameron@uthscsa.edu (I.L. Cameron).

0301-4622/02/$ - see front matter © 2002 Elsevier Science B.V. All rights reserved.
PII: S0301-4622(02)00036-4

[3,9–14]. These same xanthines bind with DNA intercalators through an interaction referred to as *polarization bonding* [15]. Polarization bonding is the $\pi-\pi$ interaction and stacking of two planar molecules, where one is polarizing (xanthine) and the other is *polarizable* (DNA intercalator). The binding of these carcinogens to certain xanthines has been shown to inhibit or reduce their binding to dsDNA [12,13,16,17]. Planarity has been described as a necessary requirement for polarization bonding complexation [15,18–23], as well as for intercalation into dsDNA [16,24–27]. Polarization bonding has been proposed as the mechanism for the bonding of carcinogenic polyaromatic hydrocarbons, such as benzo(*a*)pyrene and dimethyl benzanthracene to the purine bases adenine and guanine within dsDNA, as well as to other xanthine-like molecules [24,25]. The specific mechanism by which xanthine-like molecules inhibit polyaromatic DNA intercalating agents (DNA-IAs) from intercalation into dsDNA, has been suggested to be due to the formation of a polarization bonding complex between the xanthine and the DNA-IA [8–11,14].

Review of the literature [3,10–13,17,28–30] suggests that caffeine (CAF), a widely ingested xanthine, may be able to reduce the cytostatic/cytotoxic activity of agents that share three properties: (1) they are planar polyaromatic molecules; (2) they interact with DNA by intercalation; and (3) they form polarization bonding complexes with CAF [9,31]. When added simultaneously with or immediately before the DNA-IA, CAF has also been reported to diminish the cytotoxic and/or cytostatic effects of the DNA-IA cancer chemotherapeutic drugs doxorubicin and novantrone, in a variety of cell lines [10,11]. Additionally, CAF reduced the cytotoxicity of the DNA intercalator, ethidium bromide, by reducing its ability to enter cells [32]. The mechanism responsible for the reduction of the cytostatic/cytotoxic effects of these DNA-IAs may be the formation of polarization bonding complexes between CAF and the DNA-IA, rendering the DNA-IA less available for intercalation into the DNA. It is anticipated that a better understanding of the role of polarization bonding between intercalating agents, xanthines, and DNA will open avenues for practical applications and therapies.

An objective of this study was to better understand the mechanisms that influence CAF complexation with the DNA intercalator acridine orange. Acridine orange (AO) was chosen as a representative DNA intercalator because of its known spectral and self-aggregation characteristics, and its wide use as a fluorescence chromophore marker for both DNA and RNA [33–36]. Purified herring sperm dsDNA was chosen for study as the DNA target for AO intercalation due to its availability, purity, and biological relevance.

The specific aims of this study were to determine the effect of reactant concentration and charge modification under conditions of dynamic equilibrium on: (1) the self-association of AO; (2) the competitive complexation of AO with a potential interceptor molecule CAF; and (3) the intercalation of AO into highly polymerized DNA. This report provides information that is used to interpret fluorescence intensity results from studies that combine AO, CAF, and dsDNA.

2. Experimental

2.1. Chemicals and preparation of stock solutions

Acridine orange (AO; 3,6-bis(dimethylamino)acridine hydrochloride, >99% purity, caffeine (CAF; 1,3,7-trimethyl xanthine, >99% purity, Aldrich Chemical Company, Milwaukee, WI, USA), sodium chloride (NaCl; >99% pure, Sigma Chemical Company, St. Louis, MO, USA), HEPES buffer (1.0 mol solution, Mediatech, Inc., Herndon, VA, USA), and highly polymerized herring sperm deoxyribonucleic acid sodium salt (dsDNA; ACRØS Organics, Pittsburgh, PA, USA) were used without further purification. The purity of the dsDNA was verified by absorbance spectroscopy. ($A_{260}/A_{280}>2.0$ and $A_{260}/A_{230}>2.0$). Stock solutions of CAF and AO were prepared at a concentration of 50 mmol. A stock solution of herring sperm DNA was prepared fresh the day of use. The concentration calculations used for dsDNA were based on the method by Shoyab [17]. This method assumed that each purine and pyrimidine base occurs equally within

the DNA. Stock solutions of DNA were prepared at a concentration of 5 mmol and concentration was verified by optical density at 260 nm. All solutions and subsequent dilutions were prepared by dissolving the appropriate weighed amount in 5.0 mmol HEPES that was adjusted to pH 7.0 with 0.1 mol NaOH. Acridine orange was prepared in a stock solution at a concentration of 50 mmol in 5 mmol HEPES buffer (1.0 mol solution, Mediatech, Inc., Herndon, VA, USA).

2.2. Determination of complex formation and K_{assoc} by absorbance spectrophotometry

Optical titrations (serial additions of CAF or dsDNA to a solution of AO) were performed on a Beckman DU-600 Scanning Spectrophotometer (Beckman Instrument Co., New York, NY, USA), using a 3-ml (1-cm light path) quartz cuvette containing 2.0 ml of AO solution at a specified concentration. The DU-600 Spectrophotometer was blanked with 2 ml of a pH 7.0 buffered 5 mmol HEPES solution over the full range of wavelengths to be scanned prior to sample analysis. This effectively eliminated the need to subtract the background absorbance from the HEPES buffer. Optical absorbance scans were performed over a wavelength range from 400 to 550 nm. Neither CAF nor dsDNA produces absorbance spectra above 400 nm. The AO solution was scanned before the start of each titration series to quantitatively monitor any changes in the absorbance spectrum. Optical absorbance experiments were performed using aliquots varying in volume from 1 to 20 μl taken from the prepared stock solutions (50 mmol), and titrated into the cuvette containing 2.0 ml of the AO solution. The solution in the cuvette was then thoroughly mixed by shaking for 10 s before scanning. All titrations were performed at room temperature (25 ± 1 °C). The absorbance spectra were measured in 1-nm intervals and stored in digital format. Digitized scan data were converted to a spreadsheet file (Lotus™) using a conversion program supplied by the manufacturer (Beckman Instruments Inc.) for further analysis. Spectral data for each titration were combined and expressed in graphic form (Excel™) (*x*-axis = wavelength in nm; *y*-axis = optical absorbance) for each AO titration with AO. Initial absorbance data were corrected for the dilution due to the addition of CAF by multiplying the absorption value by an adjustment factor determined by the volume of aliquot added [9]. This manipulation slightly increased the absorption value to offset the effects of dilution. Adjusted absorption values were plotted and compared to spectra from non-complexed AO. This allowed for the visualization of an expected spectral shift that occurs when AO forms a complex.

When the CAF caused a spectral shift, a difference absorbance plot or *delta plot* was obtained. Delta plots were constructed by subtracting the adjusted absorption spectrum of AO in the presence of the xanthine from the initial spectrum of AO alone at each wavelength and for each aliquot of the titration. This procedure allowed for the creation of difference absorption values or *delta absorption values.* Delta absorption values obtained in this manner (*y*-axis = delta absorption) were plotted against wavelength in nm (*x*-axis). The determination of a single isobestic point was indicative of only two species in solution, AO, and an AO complex. Graphic representation allowed for the selection of a wavelength with the maximum sensitivity for determining the association constant [37]. This wavelength was characterized by the greatest positive response in delta absorbance values observed upon addition of each aliquot of xanthine to the AO solution. The AO-xanthine association or binding constant was determined by the following equilibrium expression:

$$I + X = IX \tag{1}$$

where I represents the intercalator (AO), X represents the interceptor molecule (xanthine), and IX represents the AO-xanthine complex, respectively. This leads to the following equation for the association constant (K_{assoc}):

$$\Delta A = KD[X]/\big(1 + K[X]\big)P_0 \tag{2}$$

where ΔA is the change in absorption after addition of a xanthine ($\Delta A \cong [IX]$) and becomes the *y*-axis of the delta plot; D is the delta extinction coefficient (also obtained from the fit); $[X]$ is the xanthine concentration (molar) in the cuvette following each aliquot addition; P_0 is the concentra-

tion of the intercalator (AO) in moles; and K is the association constant (K_{assoc}). To solve for K, Eq. (2) thus becomes:

$$Y = K(\Delta A_{\max})[X]/\big(1 + K[X]\big) \quad (3)$$

The resulting ΔA values (y-axis $= \Delta A$) were plotted against the final xanthine concentration (x-axis $= [X]$) at the $\lambda_{\max}$ that exhibited the greatest sensitivity for monitoring the formation of the AO–xanthine complex. The $\Delta A_{\max}$ value is the maximum absorbance of the complex at saturation and is equivalent to the delta extinction coefficient multiplied by the concentration of substrate (i.e. AO), and can be expressed as $D[P_0]$. The $\Delta A_{\max}$ value used to calculate the binding association constant [Eq. (3)] was iterated from the initial AO spectrum to maximize the correlation coefficient of the non-linear analysis (R^2), while not deviating significantly from the model. This method differs from a two-parameter fit (i.e. both K and $\Delta A_{\max}$ are floated) by iterating a variety of $\Delta A_{\max}$ values manually before selecting a value that maximizes the best fit of the data to the K_{assoc} curve. Fits to the association curve were determined and a graph created by non-linear least square analysis with Prism™ software (San Diego, CA, USA). The value of the association constant (K_{assoc}) with a standard error was determined from this plot. (See Connors [38] for a review and discussion of the formulas described above.)

Spectrophotometric analyses of AO with dsDNA were conducted as described above for AO-CAF, as well as an additional series of titrations performed at an AO concentration of 100 μmol. Aliquots of dsDNA were added from a 5-mmol stock solution of DNA and optical absorbance values were adjusted to account for dilution. Delta absorbance values were obtained by subtracting the optical absorbance values from the spectrum containing the lowest amplitude of absorbance found for all wavelengths between 450 and 525 nm. This base spectrum was used in lieu of the initial spectrum containing only AO. The $\Delta A_{\max}$ value used to calculate the binding association constant [Eq. (3)] was iterated from an initial value taken from this spectrum. The DNA concentration of this spectrum was subtracted from the DNA concentration of all subsequent spectra.

2.3. Fluorescence analysis by 96-well plate reader and determination of K_{assoc} values

Fluorescence analysis was performed on a range of AO concentrations from 0.5 to 10 μmol using a computer coupled Perkin–Elmer Model HTS 7000 Bio Assay Reader (Perkin–Elmer Corp., New York, NY, USA). Experiments were conducted using Serocluster 96-well EIA flat bottom plates (Costar, Data Packaging Corp., Cambridge, MA, USA) to contain the test solutions. Minimum volumes analyzed were 100 μl and aliquots were added at 50-μl increments. Fluorescence excitation was performed at 485 ± 10 nm, and fluorescence was monitored at emission wavelengths of 530 ± 12.5 and 635 ± 15.7 nm using fluorescence filters. Optical gain was set at 55 to allow for uniformity between experiments. Fluorescence values were downloaded from spreadsheet files and transformed into graphed form using Microsoft Excel™ 97 and/or Prism™ software.

Association constants were calculated using a modification of an equation described by Zaini et al. [39] to determine equilibrium constants for weakly bound complexes by absorbance spectrophotometry. By definition $K = X_d/(X_m \times X_m)$, where K is the binding constant K_{assoc}, X_d is the concentration of the AO dimer, and X_m is the concentration of the AO monomer. Conservation of mass gives $X_t = X_m + 2X_d$, where X_t is the total concentration of AO in solution. Rearranging the conservation of mass equation gives $X_m = X_t - 2X_d$, and substituting into the equation for K_{assoc} and rearranging gives Eq. (4):

$$K_{\text{assoc}}\big((X_t \times X_t) - 4(X_t \times X_d) + 4(X_d \times X_d)\big) - X_d = 0 \quad (4)$$

Rearranging gives:

$$\big((X_d \times X_d) - X_t + 1/(4 \times K_{\text{assoc}})\big) \times X_d + (X_t \times X_t)/4 = 0 \quad (5)$$

Applying the quadratic formula $\{X = [-B \pm \text{SQRT}(B^2 - 4AC]/2A\}$ to Eq. (5) and taking the only physically reasonable root gives Eq. (6):

$$X_d = \Big[X_t + 1/(4 \times K) - \text{SQRT}\big(X_t/(2 \times K) + 1/(16 \times K \times K)\big)\Big]/2 \quad (6)$$

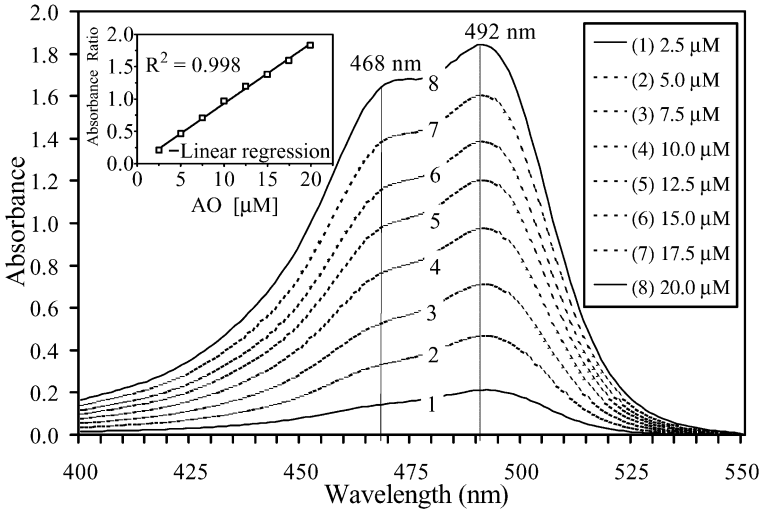

Fig. 1. The optical absorbance spectra of AO shown at various concentrations. Absorbance was scanned over a range of wavelengths between 400 and 550 nm in a (5 mmol) solution of HEPES buffer at pH 7.0. The concentration of AO for each spectrum is indicated in the legend by number. Inset: the inset figure is a linear regression analysis depicting the ratio of absorbance at 492 nm (A_{492}) to the absorbance at 468 nm (A_{468}), as a function of AO concentration.

The fluorescence values at $\lambda_{em}=530$ nm (F_{530}) is a function of X_t and $F_{530}=X_d\times\varepsilon$, where '$\varepsilon$' is the fluorescence yield of the dimer. The equation was solved by non-linear least squares using Prism™ software and binding constants determined. Concentrations of the reactants were adjusted for dilution whereas AO concentrations are reported without adjustment for dilution. Fluorescence values (f_i) are reported as raw data normalized to scale and not adjusted by a dilution factor following aliquot additions. (Note, absorbance data taken at 468 nm was also used to calculate the K_{assoc} for the AO–AO dimer using Eq. (6).)

2.4. Spectrofluorometric characterization of acridine orange bonding

AO is known to exhibit two λ_{max} fluorescence peaks, depending upon the type of interaction it has with itself or other compounds [9,40,41]. For example, when AO intercalates into DNA, presumably by forming a $\pi-\pi$ interaction or stacking complex, it has a characteristic green fluorescence maximum at approximately $\lambda_{em}=526$ nm. Alternatively, when AO associates with other compounds electrostatically (ionic) through charge transfer it has a characteristic fluorescence maximum at approximately $\lambda_{em}=650$ nm. The two emission wavelengths used in this study, $\lambda_{em}=635$ and 530 nm, represent the approximate λ_{max} for the fluorescence emission of AO when electrostatically associated with other compounds ($\lambda_{max}=$ 635 nm) and in a stacked ($\pi-\pi$) association with itself or another compound or compounds ($\lambda_{max}=$ 530 nm).

3. Results

3.1. Physiological concentrations of NaCl and higher concentrations of acridine orange facilitate the self-association of acridine orange

Optical absorbance of AO at various concentrations indicates that AO dissolved in 5 mmol HEPES solution buffered at pH 7.0 has two spectral peaks, Fig. 1. AO at a concentration of 2.5 μmol exhibits a distinct spectrum with a λ_{max} of 492 nm. At increasing concentrations of AO, a secondary spectral peak at 468 nm became more distinct and increased in amplitude. When the ratio of the absorbance value at 492 nm over the

absorbance values at 468 nm was plotted vs. AO concentrations ranging from 2.5 to 20 μmol, a significant linear correlation ($R^2=0.99$) resulted (see inset of Fig. 1). These results conform to the absorbance maximums reported by Kapuscinski and Darzynkiewicz [34] where the absorbance maxima for AO were 492 nm for the monomeric (electrostatic/charged) form, and 466 nm for the dimeric ($\pi-\pi$ stacking) form.

The fluorescence characterization of AO at low concentrations (0.5–10 μmol) is illustrated in Fig. 2a. The results also indicate the effect of a physiological concentration of NaCl (150 mmol) on the fluorescence of AO at both $\lambda_{em}=530$ (green) and 635 nm (red) over a range of AO concentrations from 0.5 to 10.0 μmol. At an AO concentration of between 5 and 6 μmol, the amplitude of green fluorescence at $\lambda_{em}=530$ nm increases abruptly. The red fluorescence ($\lambda_{em}=635$ nm) also increases abruptly between 5 and 6 μmol. However, the magnitude of the increase at $\lambda_{em}=635$ nm is proportionally less than that found at $\lambda_{em}=530$ nm. As the concentration of AO increases from 5 to 6 μmol, the changes in mean fluorescence values were highly significant, changing from 457 ± 16 to 5197 ± 289 at $\lambda_{em}=530$ nm, and from 174 ± 4 to 1371 ± 41 at $\lambda_{em}=635$ nm ($n=4$). At AO concentrations from 0.5 to 5 μmol, the addition of NaCl (150 μmol) significantly increases green fluorescence at $\lambda_{em}=530$ nm (see Fig. 2b), whereas no significant change in the mean fluorescence values was observed at $\lambda_{em}=635$ nm. Additionally, the presence of 150 mmol NaCl has no significant effect on the fluorescence intensity of AO at either $\lambda_{em}=530$ or 635 nm at AO concentrations of 6 μmol and above.

Association constants were calculated for AO self-association by assuming that the fluorescence values derived at $\lambda_{em}=530$ nm reflect the extent of dimer formation. Association constants (K_{assoc}) were calculated from the change in mean fluorescence values (delta fluorescence) at $\lambda_{em}=530$ nm (see Fig. 2b). At AO concentrations from 0.5 to 5 μmol, K_{assoc} was determined to be $37\,410\pm4758$ mol^{-1} ($R^2=0.97$) in the absence of NaCl, and $118\,000\pm16\,120$ mol^{-1} ($R^2=0.98$) in the presence of 150 mmol NaCl (see Fig. 2b). For AO concentrations >5 μmol, the association constants were determined to be $31\,500\pm756$ mol^{-1} ($R^2=0.96$) for AO alone, and $31\,380\pm697$ mol^{-1} ($R^2=0.96$) for AO in the presence of NaCl (data not shown). This indicates a significant AO concentration-dependent difference in the association con-

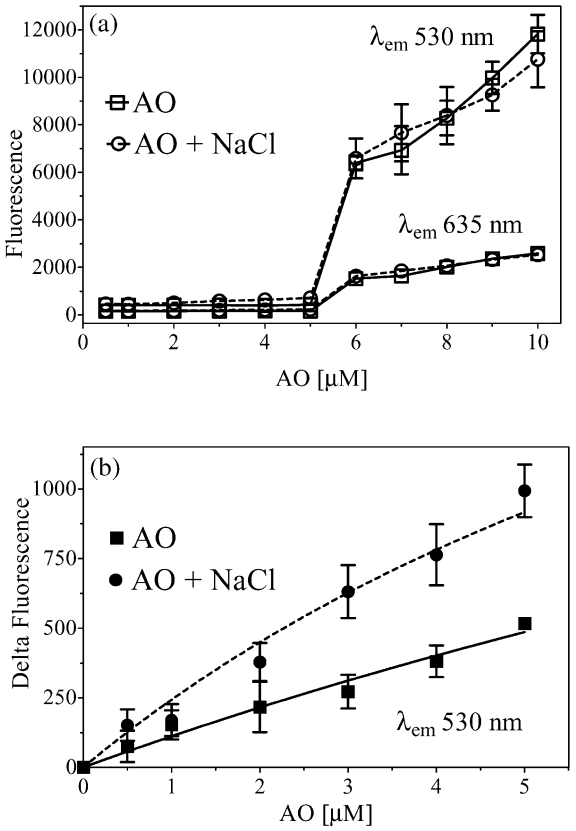

Fig. 2. Spectrofluorometric analysis of AO at concentrations ranging from 0.5 to 10.0 μmol in the absence and presence of 150 mmol NaCl. (a) Spectrofluorometric analysis was performed at $\lambda_{ex}=485$ nm, and emission was observed at $\lambda_{em}=530$ and 635 nm. Error bars shown denote standard deviation unless obscured by legend symbols ($n=4$). (b) The graph depicts the binding plot calculated at $\lambda_{em}=530$ nm for the molecular association of AO with without and in the presence of NaCl. The association constants (K_{assoc}) for AO derived from these two plots are $118\,000\pm16\,120$ mol^{-1} ($R^2=0.98$), in the presence of NaCl (150 mmol) and $37\,410\pm4758$ mol^{-1} ($R^2=0.97$) in the absence of NaCl. The fluorometric parameters were as described. Error bars denote standard deviation unless hidden by legend symbols ($n=4$).

stant in the presence of 150 mmol NaCl at low AO concentrations (<5 μmol), but not a significant difference at AO concentrations above 5 μmol.

3.2. Absorbance and fluorescence of caffeine with acridine orange at equilibrium conditions in the absence and presence of 150 mmol NaCl

To determine the association constant for the AO–CAF complex, delta absorbance values were taken at $\lambda_{max}=511$ nm and plotted against the concentration of CAF according to the methods of Larsen et al. [9]. The calculated K_{assoc} for the AO–CAF complex was found to be 255 ± 5 mol^{-1}. The AO–CAF binding plot fit well ($R^2=0.997$) to a model in which AO and CAF form a 1:1 complex as previously reported [9].

Spectrofluorometric analysis was performed at an AO concentration of 2 μmol to determine the effect of CAF and a physiological concentration of NaCl on the fluorescence spectra of AO. CAF was added over a series of CAF/AO molecular ratios ranging from 2500:1 to 0.5:1, and the fluorescence intensity determined at $\lambda_{em}=530$ and 635 nm. The fluorescence intensity was again determined following the addition of NaCl to a final concentration 150 mmol and pH 7.0 to each test well containing both AO and CAF.

The data in Fig. 3a depict the mean fluorescence values at $\lambda_{em}=530$ nm of 2 μmol AO with CAF in the absence of, and in the presence of, 150 mmol NaCl over a range of CAF/AO molecular ratios from 0.5 to 10.0 (1–20 μmol CAF). The initial fluorescence values for AO at a concentration of 2 μmol with and without 150 mmol NaCl, differed significantly prior to titration with CAF. Specifically the presence of NaCl in the 2 μmol AO solution significantly increased the fluorescence value at $\lambda_{em}=530$ nm from a mean of approximately 400 to approximately 500. However, upon the addition of increasing amounts of CAF, the mean fluorescence values increased significantly over the initial mean fluorescence values. The addition of 150 mmol NaCl to the series of AO–CAF solutions did not significantly effect ($P>0.05$) the mean fluorescence values over the full range of CAF concentrations tested up to a CAF/AO ratio of 1000:1 (data not shown). However, at the CAF concentration of 5 mmol (molecular ratio = 2500:1), there was a significant change

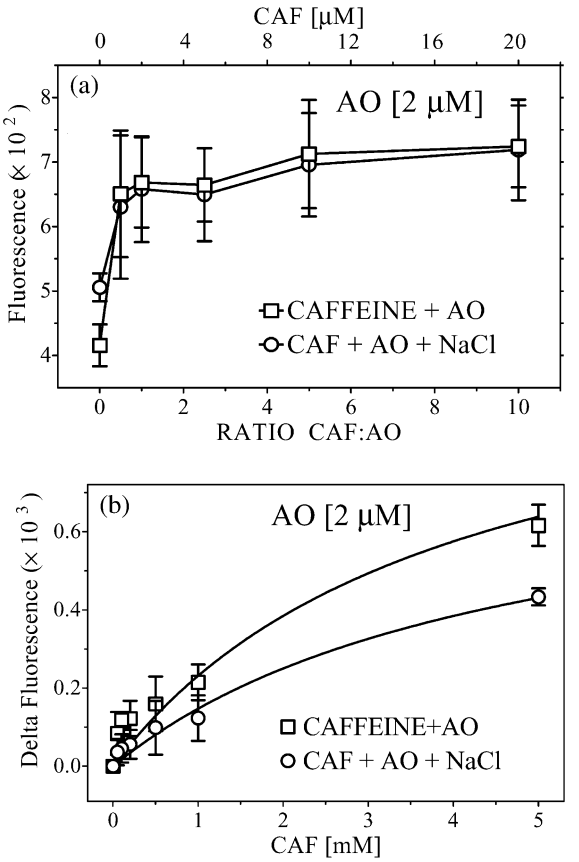

Fig. 3. Effect of CAF and NaCl on the fluorescence of AO and the formation of the AO–CAF complex. (a) A plot of fluorescence intensity of AO excited at $\lambda_{ex}=485$ nm and monitored at $\lambda_{em}=530$ nm vs. CAF concentration to show the effect of CAF and NaCl on the fluorescence of AO and the formation of the AO–CAF complex. Solutions of 2 μmol AO were analyzed using spectrofluorometric techniques in the presence of various concentrations of CAF, with and without addition of NaCl (150 mmol). Error bars indicate standard deviation unless hidden behind the symbol ($n=3$). (b) Association curves were plotted from net fluorescence values (minus background fluorescence) vs. CAF concentration. This delta fluorescence plot was used to determine K_{assoc} for the AO–CAF complex at an AO concentration of 2 μmol in the absence and presence of 150 mmol NaCl. K_{assoc} for the AO–CAF complex at 2 μmol AO was found to be 254 ± 27 mol^{-1} ($R^2=0.89$) in the absence of 150 mmol NaCl, and 216 ± 20 mol^{-1} ($R^2=0.93$) in the presence of NaCl.

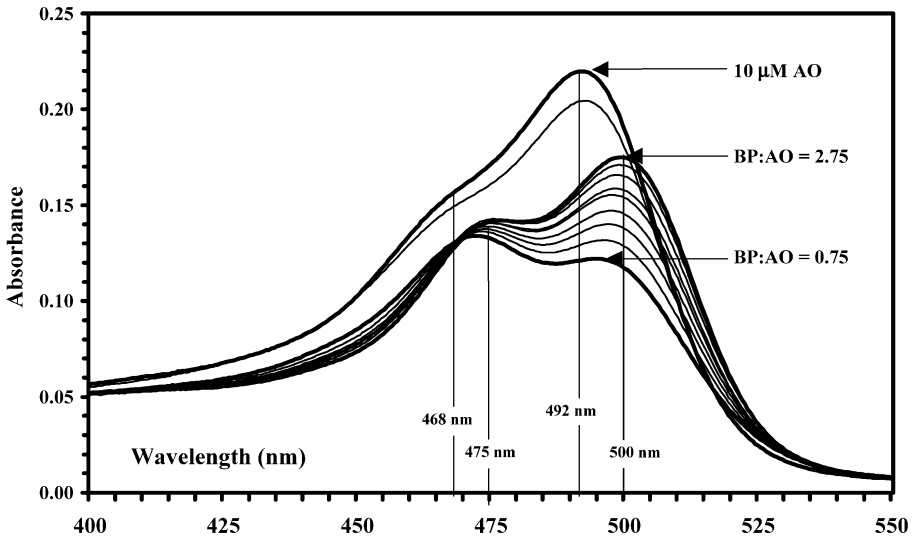

Fig. 4. Optical absorbance spectra taken from a series of titrations of 10 μM AO with different concentrations of dsDNA. The dsDNA BP/AO ratio of selected spectra denoting important transitions within the titration series are denoted with bolder lines. Some of the spectral series is not shown to simplify the data presentation. At BP/AO ratios between 0.0 and 0.75, prevalent peaks occur at λ_{abs} of 468 and 492 nm. These peaks correspond to the prevalent absorbance peaks found at concentrations of AO at 10 μmol or above. The absorbance spectra from BP/AO ratios above 0.75 denote a definitive red-shift in absorbance with the simultaneous creation of two distinct peaks at 475 and 500 nm, respectively.

in the mean fluorescence intensity with the value going from 1245 ± 53 for CAF and AO alone to 1150 ± 34 with the addition of 150 mmol NaCl (data not shown). The gradual change in fluorescence intensity at $\lambda_{em} = 530$ nm went from a mean value of 671 ± 109 ($n = 3$) at a CAF/AO ratio of 0.5 (1 μmol CAF), to a value of 1245 ± 53 at a molecular ratio of 2500 (5 mmol CAF). The mean values in fluorescence intensity that resulted with the addition of either CAF or CAF with NaCl to AO (2 μmol) did not significantly differ from each other in mean fluorescence values at $\lambda_{em} =$ 635 nm for all test conditions (data not shown). Mean spectrofluorometric values were plotted against CAF concentration (see Fig. 3b) to determine an association constant (K_{assoc}) for the AO–CAF complex in the absence and presence of 150 mmol NaCl. The association constant for the formation of the AO–CAF complex at an AO concentration of 2 μmol was determined to be 254 ± 27 and 216 ± 20 mol^{-1} in the absence and presence of NaCl, respectively.

3.3. Association of acridine orange with dsDNA: evidence for multiple acridine orange binding sites on dsDNA

Experiments were undertaken to characterize the interaction of AO with DNA over a range of DNA base pairs (BP)/AO ratios in the absence and presence of a physiological concentration of NaCl. As the ratio of BP to AO increased from approximately 0.4 to 0.65, an overall drop in absorbance values between the wavelengths of 450 and 525 nm occurred (Fig. 4). With continued additions of aliquots of DNA, the absorbance peak near 468 nm is still apparent while the initial main absorbance peak at 492 nm is no longer detectable. With the continued additions of aliquots of DNA and the subsequent increase in the BP/AO ratio above 0.65, the absorbance at $\lambda_{abs} = 475$ nm began to increase and to display a red shift from 468 to 475 nm. This spectral peak at $\lambda_{abs} = 475$ nm gradually increased in height with increasing DNA concen-

Table 1
Summary and description of optical absorbance maxima peaks observed during the titration of 100 μM AO with dsDNA, and the range of BP/AO molecular ratios over which these absorbance peaks were observed during the titration series

λ_{max} abs. (nm)	BP:AO ratio
468	<0.09–2.99
475	1.72–9.13
492	<0.09–0.53
500	0.97–9.13

tration before reaching an absorbance plateau at BP/AO ratios of 3.0 and above. Additionally, at BP/AO ratios of approximately 1.72, another absorbance peak near $\lambda_{abs}=500$ nm increased in amplitude with each additional aliquot of DNA. This absorbance at $\lambda_{abs}=500$ nm steadily increased throughout the range of titrations from a BP/AO ratio of 1.72–9.13. Table 1 is a summary and description of the optical absorbance peaks observed during the titration of 100 μmol AO with dsDNA and the range of BP/AO molecular ratios over which these absorbance peaks were observed during the titration series.

Spectral data from the titration of AO with dsDNA performed at a concentration of 10 μmol AO were used to generate the delta absorbance plot shown in Fig. 5. The results indicate a single isobestic point at 470 nm. The association constant was calculated from a plot of delta absorbance values at 503 nm vs. DNA concentration (see inset Fig. 5). The K_{assoc} from this plot was 3766 ± 131 mol^{-1}.

In addition to the optical absorbance of AO and dsDNA, a spectrofluorometric analysis of the interaction of AO with dsDNA at $\lambda_{ex}=485$ nm, and $\lambda_{em}=530$ and 635 nm was also conducted. The interaction of DNA with lower concentrations of AO (2 μmol) mimicked the results found at the higher AO concentration of 20 μmol for BP/AO ratios of 4:1 and above (data not shown). The association curve for AO over a series of steadily increasing DNA concentrations ranging from 8 to 250 μmol of DNA is shown in Fig. 6. The delta fluorescence values were obtained by subtracting the background fluorescence of HEPES buffered AO at 2 μmol in the absence of DNA. The

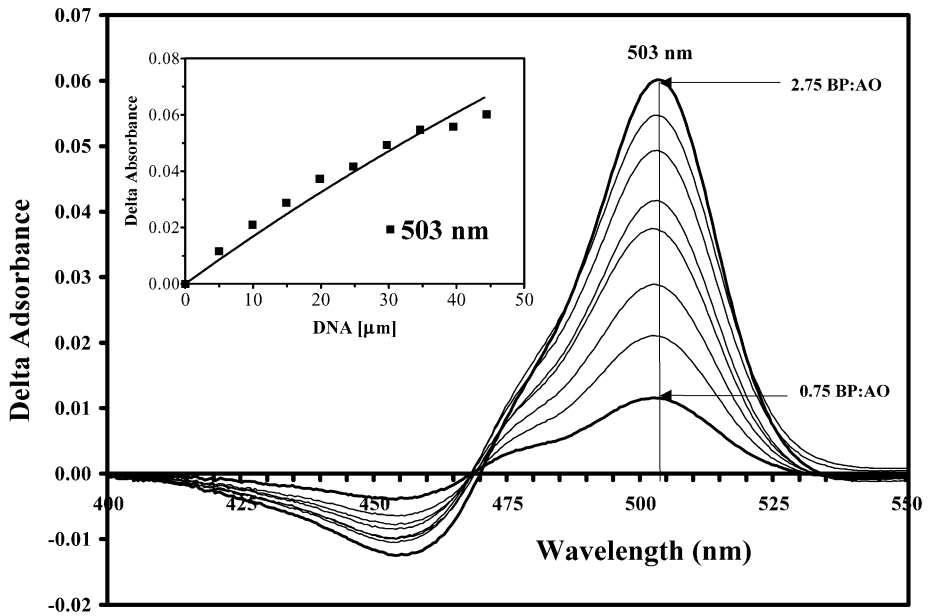

Fig. 5. Delta absorbance plot of 10 μM AO titrated with herring sperm dsDNA. Actual DNA concentrations ranged from 5 to 55 μmol. The inset figure shows delta absorbance values taken at 503 nm plotted against the DNA concentration.

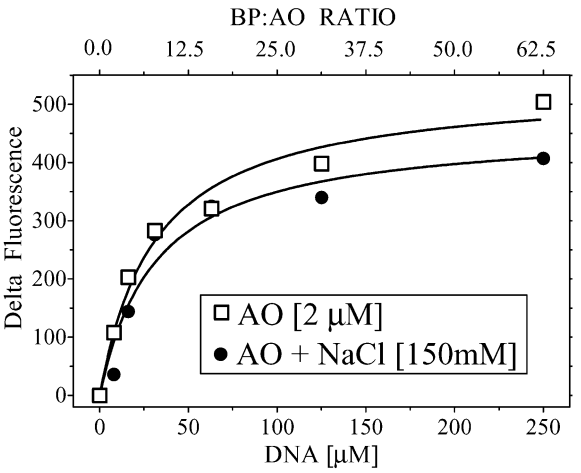

Fig. 6. Spectrofluorometric analysis of AO (2 μmol) with various concentrations of herring sperm DNA in the presence and absence of NaCl (150 mmol). The effect of NaCl on the fluorescence of 2 μmol AO was determined over a range of BP/AO ratios from 4 to 62.5. The excitation wavelength was 485 nm while emission was monitored at 530 nm. The association constant was determined for 2 μmol AO with DNA to be 3199 ± 310 mol^{-1} ($R^2 = 0.98$) in the absence of NaCl, and 3169 ± 498 mol^{-1} ($R^2 = 0.96$) in the presence of NaCl. Error bars are shown to denote confidence intervals at 95% unless hidden by a data point symbol.

association constant obtained for the interaction of AO with DNA using spectrofluorometric methods was $31\,990 \pm 3190$ mol^{-1}. As also illustrated in Fig. 6, the addition of 150 μmol NaCl to the initial 2 μmol AO solution, had little if any effect on the binding constant between AO and the dsDNA resulting in a value of $31\,690 \pm 4980$ mol^{-1}.

Experiments were conducted to determine the effect of physiological concentrations of NaCl on the fluorescence intensity of the AO–DNA complex. Fig. 7 depicts the spectrofluorometric analysis of AO at concentrations ranging from 0.5 to 10.0 μmol with 20 μmol DNA, in the presence or absence of 150 mmol NaCl. Samples were excited at a wavelength of 485 nm, and fluorescence emission values were read at $\lambda_{em} = 530$ and 635 nm. Spectrofluorometric analyses of 20 μmol DNA at AO concentrations ranging from 0.5 to 3.0 μmol revealed a slight, but significant increase in fluorescence values at $\lambda_{em} = 530$ nm over this concentration range of AO. The addition of NaCl (150 μmol) to the experimental environment containing AO and DNA, did not contribute significantly to the fluorescence values at either $\lambda_{em} =$ 530 or 635 nm until AO concentrations exceeded 2 μmol as determined by ANOVA statistics. At AO concentrations > 3.5 μmol, the fluorescence values of the DNA solution at $\lambda_{em} = 530$ nm in the absence and presence of NaCl increased four- and five-fold, respectively. In the absence of NaCl, the plot of fluorescence values at $\lambda_{em} = 530$ nm plateaus at AO concentrations ranging from 4.0 to 7.0 μmol. Also, the data in Fig. 7 reveal that the fluorescence values in the presence of 150 mmol NaCl over the AO concentration range 4.0–7.0 μmol, differed significantly (were increased) from the values obtained at $\lambda_{em} = 530$ nm in the absence of NaCl. At $\lambda_{em} = 635$ nm, fluorescence values increased slightly between AO concentrations of 3.5–4.0 μmol and continued to gradually rise with increasing concentration of AO. Unlike the results obtained at $\lambda_{em} = 530$ nm, the presence of or the absence of NaCl had no significant effect on the fluorescence at $\lambda_{em} = 635$ nm.

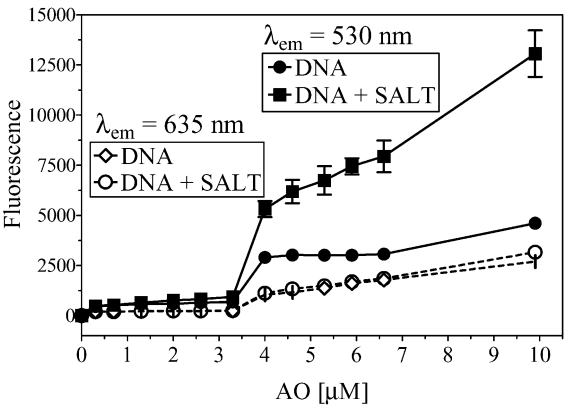

Fig. 7. Spectrofluorometric analysis of 20 μmol DNA in the presence of concentrations of AO ranging from 0.5 to 10.0 μmol, in the absence and presence of 150 mmol NaCl. Spectrofluorometric analysis was performed at $\lambda_{ex} = 485$ nm, and emission was observed at $\lambda_{em} = 530$ and 635 nm. Error bars shown denote standard deviation unless hidden by legend symbols ($n = 4$).

Table 2
The effect of 150 mmol NaCl, 5 mmol caffeine, and/or 2 mmol DNA on the fluorescence intensity at λ_{em} 530 nm of a 2-μmol AO solution

Reactants (2 μmol AO)	Without NaCl Mean ± S.E. (SNK)	With NaCl (150 mmol) Mean ± S.E. (SNK)
AO	514.0 ± 6.5 (A)	635.5 ± 17.7 (B)
AO + CAF	661.0 ± 19.3 (B)	701.3 ± 53.7 (B)
AO + DNA	988.0 ± 11.1 (E)	795.0 ± 17.7 (C)
AO + DNA + CAF	880.3 ± 27.6 (D)	793.7 ± 14.4 (C)

Fluorescence (λ_{ex} = 485 nm and λ_{em} = 530 nm) was measured for AO (2 μmol) in the absence of, and in the presence of NaCl (150 mmol), caffeine (5 mmol), and DNA (2 mmol) alone or in combination. Significant differences were found by one-way ANOVA ($P \leq 0.05$). The Student–Newman–Keuls (SNK) multiple range test revealed a significant difference between means ($P < 0.05$), as indicated in the table. Statistical means having a different letter designation are statistically different ($P < 0.05$), while those means having the same letter are not significantly different ($P > 0.05$). (Note: experiments with AO and NaCl, $n = 4$; all other experiments, $n = 3$.)

3.4. Spectrofluorometric study of effects of 150 mmol NaCl on the interactions of acridine orange with itself, with caffeine, and with dsDNA

Experiments were performed to determine the influence of NaCl at physiological concentrations on the interactions of AO with itself, AO with CAF, and AO with dsDNA. It was hypothesized that the addition of salt might affect the K_{assoc} values of AO and the other reactants by modifying the charge on the reactants and/or decreasing the influence of water molecules. To minimize AO self-association, i.e. dimerization, a relatively low concentration of AO (2 μmol) was used throughout this series of experiments. The interaction between reactants was analyzed by spectrofluorometric methods at λ_{ex} = 485 nm and monitored at λ_{em} = 530 nm (green).

Solutions of 2 μmol AO alone and in various combinations with 150 mmol NaCl, 5 mmol CAF, and 2 mmol DNA were studied. Table 2 summarizes the results and the statistical analysis for difference. The results, as reported in Table 2, fell into distinct groups with statistically different means ($P < 0.05$). The lowest mean fluorescence value of 514.0 was produced by 2 μmol AO alone. Addition of 150 mmol NaCl to 2 μmol AO caused a significant increase in the mean fluorescence value from 514.0 to 635.5. This value of 635.5 was not significantly different from either the mean fluorescence value of 661.0 determined for AO in the presence of 5 mmol CAF, or the mean fluorescence value of 701.3 determined for AO in the presence of both 5 mmol CAF and 150 mmol NaCl. The addition of 2 mmol DNA to the 2 μmol AO solution caused the highest mean fluorescence value of 988.0, which was almost double the mean fluorescence value of 514.0 determined with AO alone. Yet, this value of 988.0 was significantly higher than the value of 795.0 obtained with the addition of 150 mmol NaCl to the AO–DNA solution.

Further manipulation of the AO–DNA solution by the addition of 5 mmol CAF significantly lowered ($P < 0.05$) the mean fluorescence value to 880.3. Yet, this value of 880.3 was significantly higher than the value of 795.0 obtained with the addition of only 150 mmol NaCl to the AO–DNA solution. The combination of 2 mmol DNA, 5 mmol CAF, and 150 mmol NaCl with AO gave a mean fluorescence value of 793.7, that was not significantly different from the mean value obtained for the same reactants in the absence of CAF with the combination of AO with DNA and 150 mmol NaCl.

Thus, the AO fluorescence at λ_{em} = 530 nm almost doubled by the addition of either 2 mmol DNA or by the addition of 5 mmol CAF, plus 2 mmol DNA compared to only a modest increase by the addition of CAF. However, the addition of NaCl to the same experimental environment further increased the fluorescence intensity of AO in the presence of CAF, but significantly reduced the ability of DNA to increase the fluorescence intensity of AO.

3.5. The competitive binding of AO to dsDNA in the presence of CAF with and without charge modification using NaCl

The following presents the results of fluorescence intensity experiments that kept all but one reactant at constant concentration while varying a single reactant, such as AO (Fig. 8), CAF (Fig. 9), or dsDNA (Fig. 10). The effect of 20 μmol

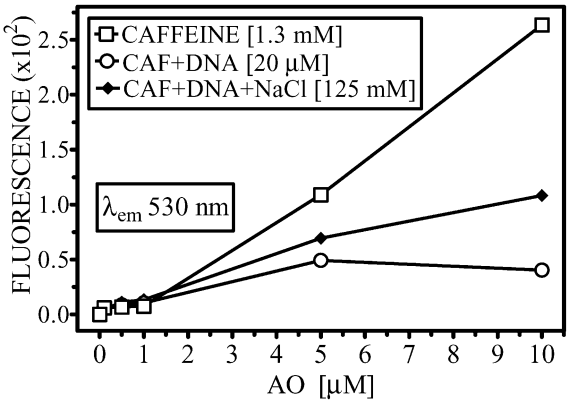

Fig. 8. The effects of 1.3 mmol caffeine on the fluorescence of AO at $\lambda_{em}=530$ nm over a series of AO concentrations ranging from 0.01 to 10 μmol, in the absence or presence of 20 μmol DNA, with and without 125 mmol NaCl. Fluorescence ($\lambda_{ex}=485$ nm) was monitored at $\lambda_{em}=530$ nm. Standard deviation bars are hidden by symbols that represent means ($n=4$).

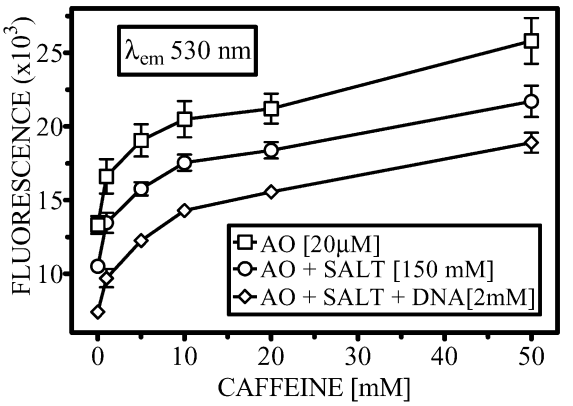

Fig. 9. The effect of 150 mmol NaCl in the absence and presence of 2 mmol DNA on the fluorescence ($\lambda_{ex}=485$ and 530 nm) of 20 μmol AO with increasing concentrations of caffeine. Error bars denote standard deviation ($n=4$).

DNA on the fluorescence intensity of a 20-μmol AO solution (1:2 BP/AO ratio) over a series of CAF concentrations in the absence and presence of 125 mmol NaCl $\lambda_{em}=530$ nm is illustrated in Fig. 9. The addition of 125 mmol NaCl to the AO–CAF solution caused a significant decrease in mean fluorescence values throughout the range of CAF concentrations. Upon the addition of 20 μmol DNA to AO solutions containing both CAF and 125 mmol NaCl, the mean fluorescence values further decreased. However, fluorescence analysis of 2 μmol AO with CAF over the same molecular ratio range of 0.5–2500 in the absence of or the presence of 125 mmol NaCl, with and without 2 μmol DNA (1:2 BP/AO ratio, data not shown) revealed no significant change in fluorescence values at $\lambda_{em}=530$ nm over a range of CAF concentrations up to 5 mmol CAF. Fluorescence values for all test conditions at $\lambda_{em}=635$ nm for both 2 and 20 μmol AO concentrations showed no significant differences (data not shown).

Experiments were conducted to determine the effect of AO concentration in the absence of or in the presence of 125 mmol NaCl on the interactions of AO with DNA and CAF. Fig. 8 is a plot of mean fluorescence values ($\lambda_{ex}=530$ nm) of AO at concentrations ranging from 0.1 to 10 μmol with 1.3-mmol CAF, in the absence and presence of 20 μmol DNA, with or without 125 mmol NaCl. The plot of the fluorescence values from the formation of the AO–CAF complex illustrates a minimal effect on fluorescence intensity at $\lambda_{em}=530$ nm until the AO concentration exceeded 1 μmol. At AO concentrations of 5 and 10 μmol, obvious differences in fluorescence intensity were observed. A similar pattern of fluorescence values occurs with 1.3 mmol of CAF in the presence of 20 μmol DNA, but the slope of the rise in

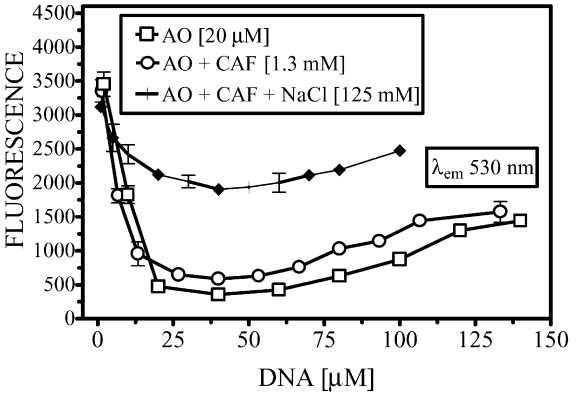

Fig. 10. Spectrofluorometric analysis at $\lambda_{em}=530$ nm of 20 μmol AO titrated with dsDNA in the absence and presence of 1.3 mmol caffeine, with and without 125 mmol NaCl. Error bars indicate standard deviation unless hidden by symbols ($n=4$).

fluorescence intensity is lower. In this case, fluorescence values at AO concentrations of 5 and 10 μmol were substantially lower. The presence of 125 mmol NaCl in the AO–DNA mixture suppresses the fluorescence intensity at AO concentrations of 5 and 10 μmol.

Spectrofluorometric analysis of 20 μmol AO at $\lambda_{em}=530$ nm was conducted with increasing DNA concentrations in the absence and presence of 1.3 mmol CAF, with and without 125 mmol NaCl (Fig. 10). In the presence of low concentrations of DNA (<40 μmol), plots of fluorescence values show a significant decrease in the mean fluorescence intensity for each of the three test conditions: AO–DNA; AO–DNA+CAF; and AO–DNA+CAF+SALT. This DNA-dependent decrease in fluorescence values with increasing concentrations of DNA reaches a minimum value at 40 μmol DNA concentration or a BP/AO ratio of 1:1. This drop in mean fluorescence values over DNA concentrations ranging from 0 to 40 μmol, was greatest for test solution containing only 20 μmol AO. The presence of 1.3 mmol CAF in the test system containing 20 μmol AO at low DNA concentrations, resulted in a more precipitous decrease in mean fluorescence intensity over the DNA concentrations <20 μmol. Finally, the addition of 125 mmol NaCl to the AO–CAF solution at DNA concentrations of 10 μmol and above, significantly suppresses the decrease in mean fluorescence values at $\lambda_{em}=530$ nm as seen for solutions containing AO alone or AO–CAF, over the same range of DNA concentrations.

To characterize the electrostatic interactions, spectrofluorometric analysis of 20 μmol AO at $\lambda_{em}=635$ nm was conducted with increasing DNA concentrations for the same experimental conditions as described in the legend of Fig. 10 (data not shown). A plot of mean fluorescence values observed at $\lambda_{em}=635$ nm from a 20 μmol AO solution over a range of DNA concentrations up to 135 μmol, revealed a significant decrease in fluorescence intensity upon the addition of low concentrations of DNA. However, as DNA concentrations increased to even higher levels (>23 μmol), fluorescence values stopped decreasing and began to increase. The apparent transition point in the plot of mean fluorescence values from decreasing values to increasing values occur at a DNA concentration of ~23 μmol or a DNA/AO molecular ratio of approximately 1:1 (i.e. 1:2 base pair/AO molecule ratio). With higher DNA concentrations, fluorescence intensity at $\lambda_{em}=635$ nm steadily increased reaching a plateau at 100 μmol of DNA (2.5:1 BP/AO). Exposure of a 1.3 mmol CAF and 20 μmol AO solution to increasing concentrations of DNA resulted in a distinctly different fluorescence plot than was observed when CAF, was absent from the mixture (data not shown). This spectral pattern with 1.3 mmol CAF present differed in two ways from the plot of AO with only DNA present. First, the transition of mean fluorescence intensity with higher concentrations of DNA occurred at a lower concentration of approximately 9 μmol of DNA or a BP/AO ratio of 0.25. Secondly, at higher DNA concentrations, the fluorescence intensity plateaus at significantly lower mean fluorescence intensity and at a DNA concentration of approximately 60 μmol of DNA (3:2 BP/AO ratio). However, when 125 mmol NaCl is present in the AO–CAF solution over the range of DNA concentrations, the large changes in fluorescence intensity as described in the two previous experimental conditions is not seen. In the two previously discussed experimental conditions of AO–DNA and AO–CAF–DNA, the quenching of mean fluorescence intensity with low concentrations of DNA does not occur when 125 mmol NaCl was present in the AO–CAF solution. The addition of NaCl to the test environment caused the mean fluorescence intensity at DNA concentrations above 40 μmol, to be significantly lower than the previous experimental conditions of AO and DNA in the absence or presence of CAF.

4. Discussion

4.1. Self-association of acridine orange

Kapuscinski and Darzynkiewicz [34] reported that the absorbance maxima for the AO monomer and AO dimer to be 492 and 466 nm, respectively. At low AO concentration, we observed a peak absorbance at 492 nm (the monomer) and at increasing concentrations of AO, a secondary peak

at 468 nm begins to increase in amplitude (Fig. 1). Spectral analyses of AO at concentrations of less than 1 μmol do not exhibit this secondary peak. The peak at 466 nm has been proposed [34,35,42–44] to be indicative of the formation of self-aggregates of AO, specifically a stacked dimer. This suggests that the formation of thermodynamically stable AO–AO dimers may occur even at a concentration below 2.5 μmol.

Bound AO is known to fluoresce at two distinct wavelengths based on the type of molecular association that occurs. When AO binds electrostatically to a compound (e.g. RNA), it has a characteristic red fluorescence with λ_{max} emission of 635 nm. Alternatively, when AO intercalates as occurs with DNA it fluoresces green at a λ_{max} = 530 nm [40]. The fluorescence of free unbound AO monomer is weak at low concentrations (1–10 μmol) and therefore contributes little to background fluorescence. The electrostatic interaction of AO with itself can therefore be monitored at λ_{em} = 635 nm, while the formation of the AO–AO stacked dimer can be followed by monitoring the fluorescent emission at 530 nm.

The equilibrium in the AO–AO system is controlled by the association constant for the formation of the AO–AO dimer. Short-range stacking interactions including hydrophobic and dispersive forces are driving this association [14]. These forces are not supposed to be affected by changes in ionic strength. At a pH close to 7, however, AO is almost completely protonated (pK_a = 10.4 at 20 °C, [45]) and this introduces a long-range electrostatic interaction to the system [33]. At AO concentrations of up to 50 μmol, the repulsive electrostatic forces limit self-aggregation of AO [33], and the process is strongly affected by electrolytes. According to Robinson et al. [33], the log K_{assoc} for AO (AO–AO dimerization constant) is proportional to the square root of ionic strength, as predicted by the Debye–Hückel theory. The increase of NaCl concentration to 150 mmol resulted in an increase in K_{assoc} from 37 410 to 118 000 mol^{-1} at AO concentrations ranging from 0.5 to 5.0 μmol.

In summary, the formation of the dimer or stacked AO aggregate is dependent upon the concentration of AO. The addition of salt to AO solutions facilitates dimer formation at lower AO concentrations, but has no significant additional effect at AO concentrations above 5 μmol. The sharp increase in green fluorescence (λ_{em} = 530 nm) at an AO concentration of 5 μmol is probably due to a shift in AO equilibrium toward the formation of AO aggregates. The critical concentration for this phenomenon seems to be approximately 5–6 μmol. Below this concentration, AO exists primarily as a monomer with an increased formation of multimeric species as the concentration of AO increases toward 5 μmol. At concentrations above 5 μmol, molecular AO exists in solution as a monomer, a dimer, and possibly as unstacked aggregates of dimers. The sharp increase in fluorescence at λ_{em} = 530 nm at 5 μmol may be attributed to the formation of AO aggregates that facilitate docking and dimerization of AO monomers. In support of this idea, note that the addition of high molecular weight DNA lowered the apparent critical concentration of AO to aggregate from 5–6 (Fig. 6) to 3.5 μmol (Fig. 7).

4.2. Interactions of caffeine with acridine orange

The optical absorbance and fluorescence results from present and past studies [9,10,14] on the interaction of AO and CAF can be explained as follows; the DNA intercalator chromophore acridine orange, exhibits optical absorbance and singlet state fluorescence emission bands in the visible region of the spectrum that are sensitive to the solvent environment of the chromophore. The observed red-shift of AO absorption and the corresponding fluorescence emission bands and increase in fluorescence intensity of AO in the presence of the trimethyl xanthine, CAF, with its three hydrophobic methyl groups, are characteristic of changes in the solvent environment associated with the intercalator in the presence of DNA [34,35]. In general, excited states arising from π–π transitions such as the optical transitions observed with AO and DNA, are expected to decrease in energy (red-shift) as the solvent becomes increasing hydrophobic [46–48]. Complexation between CAF and the DNA intercalator AO results in the replacement of water molecules solvating the intercalator by the more hydrophobic

CAF molecule. Thus, the $\pi-\pi$ excited state experiences a more hydrophobic environment and a correspondingly lower energy resulting in a red-shift in the absorbance and emission bands. In addition, the exclusion of water molecules surrounding the chromophores cause an increase in the fluorescence intensity of AO as water is an effective quencher of the excited state of the intercalator.

It appears that the primary criteria for energy minimization of the AO–CAF complex is the centering of the CAF ring system over that of the DNA intercalator ring system with only a minimal contribution from the relative orientation of side groups [9]. Previous descriptions of complex formation between CAF and DNA intercalators portray, complexes between CAF and DNA intercalators with distinctly planar ring structures [15].

4.3. Caffeine as an interceptor of the DNA intercalator AO

Caffeine has been suggested as a naturally occurring interceptor molecule for a variety of DNA intercalators. Previous results from Traganos et al. [10,11] demonstrate that CAF can modulate the effects of the DNA intercalator molecules doxorubicin (DOX), novantrone (NOV), and ellipticine (ELP) in L1210 leukemic cell line. Specifically, the addition of DOX, NOV, and ELP to L1210 cells decreases cell growth to 26, 48 and 20%, respectively, relative to control cultures. The simultaneous addition of 5 mmol of CAF together with either DOX, NOV, or ELP reduces the suppression of cell growth to only 65, 83 and 42% relative to control cultures. In addition, Traganos et al. [10,11] found that the sequence in which CAF was added affects the degree of cytotoxicity relative to cell proliferation with these mutagens. When CAF is added either before or after the mutagens, CAF afforded no protection against these mutagens. Only when CAF is added simultaneously with the mutagens are the cell-damaging effects leading to cell death reversed. Taken together, these findings imply that co-treatment facilitates the formation of a CAF–intercalator complex and that such a complex is less able to bind to DNA or otherwise affect cellular replication.

Additional evidence for CAF–intercalator complexation as a mechanism for reducing the biological effects of the intercalating agent can be found in the energy-minimized complexes of CAF with hadicine and hydroxyurea [49]. Caffeine displays a non-protective property against cellular damage caused by hydroxyurea and was shown to increase cell death in combination with hydroxyurea [49]. It should be pointed out that hydroxyurea and hadicine are aliphatics and contain no conjugated ring systems. The molecular modeling studies [9] show that the energy for complexation between hydroxyurea and CAF are much less favorable than for AO–CAF resulting in a weaker complex with a lower association constant. This phenomenon of weak complex formation is presumably due to the aliphatic nature of hydroxyurea, which is not capable of $\pi-\pi$ complex formation with CAF. The result is an effective concentration of hydroxyurea that is unaffected by the CAF in solution.

Comparison of the complexing ability of CAF relative to other DNA interceptor molecules is of interest. Optical titrations and molecular modeling calculations of mutagen–porphyrin complexes revealed binding constants and relative binding energies for these complexes. Binding constants for chlorophyllin complexes with heterocyclic amines are at least one order of magnitude higher than that of CAF with the same model intercalators [4–6,50]. This trend is also reflected in the relative binding energies determined from molecular modeling calculations [8,51]. These binding energies are a factor or two larger for mutagen–chlorophyllin complexes relative to mutagen–CAF complexes. Thus, although CAF may play a role as an interceptor molecule, its ability to prevent cell damage is predicted to be less effective than the porphyrin-type interceptors at the same molecular concentration.

In summary, the results of optical titration and spectral analysis studies of CAF with the DNA-intercalator AO demonstrates that CAF can complex with AO via a $\pi-\pi$ type interaction. The dominant force in the formation of such complexes appears to be van der Waals interactions resulting in maximal ring overlap between the two mole-

Table 3
Summary of association constants (K_{assoc}) for AO with itself, with caffeine (CAF), and with dsDNA without and in the presence of 150 mmol NaCl

Complex	Method	$K \pm$ S.D. (mol^{-1})	Concentration	Source
AO–AO	Absorbance	29 100	AO (20 μmol)	[14][a]
	plus NaCl[b]	42 500		
	Fluorescence	37 410 ± 4758	AO (0.5–5.0 μmol)	This study
	plus NaCl[b]	118 000 ± 16 120		This study
	Fluorescence	46 700 ± 1807	AO (6.0–10.0 μmol)	This study
	plus NaCl[b]	41 820 ± 3671		This study
AO–CAF	Absorbance	256 ± 5	AO (10 μmol); CAF (1–5000 μmol)	This study
	Absorbance	258 ± 5	AO (10 μmol); CAF (1–5000 μmol)	[9]
	Absorbance	258 ± 7	AO (20 μmol);	[14][a]
	plus NaCl[b]	169 ± 9	CAF (1–2000 μmol)	
	Fluorescence	254 ± 27	AO (2 μmol);	This study
	plus NaCl[b]	216 ± 20	CAF (1–20 μmol)	This study
AO–DNA	Absorbance	3766 ± 131	AO (10 μmol); DNA (>200 μmol)	This study
	Absorbance	3643 ± 56	AO (4–10 μmol); DNA (100 μmol)	This study
	Absorbance	3869 ± 27	AO (20–45 μmol); DNA (20 μmol)	This study
	Absorbance	33 510 ± 285	AO (0.1–3 μmol); DNA (100 μmol)	This study
	Absorbance	31 960 ± 316	AO (0.8–3.4 μmol); DNA (20 μmol)	This study
	Absorbance	37 660 ± 431	AO (3 μM); DNA (5–170 μM)	This study
	Fluorescence	31 990 ± 3190	AO (2 μmol); DNA (>20 μmol)	This study
	plus NaCl[b]	31 690 ± 4890		This study

[a] K_{assoc} calculated using absorbance data and a mathematical model.
[b] NaCl concentration of 150 mmol.

cules of the complex [9,15,18]. Complexation between CAF and aliphatic mutagens show much lower binding energies relative to CAF complexes with aromatic intercalators. As demonstrated in this and past studies [9], the corresponding binding constant for CAF–AO complexes is approximately 250 mol^{-1} (Table 3). These results suggest a possible role for CAF as an interceptor molecule although its interceptor property is expected to be less than for interceptor molecules with more extended conjugated ring systems (e.g. chlorophyllin) [9].

4.4. Interactions of acridine orange with dsDNA

Studies on the interaction of AO with DNA are complicated by the formation of dimers and/or higher multimers of the DNA intercalator, resulting in muti-component optical and fluorescence spectra that are difficult to analyze. The interaction of AO with DNA is complex. The fluorescence emission spectrum is affected not only by the gross structure of the DNA [52,53], but also by the concentration of AO, the pH, the presence of competing reactants, temperature and ionic strength [14]. Although it is generally assumed that the AO binding affinity, fluorescence emission wavelength and fluorescence efficiency, are all relatively insensitive to the DNA-base composition [34,52], the actual studies on synthetic DNA polymers of defined base composition and configuration are scarce and only a few polymers have been tested [35,54–56].

The spectrophotometric analysis of the AO–DNA binding reported herein suggested the presence of a single bound species at high DNA/AO ratios and therefore, only one mode of binding (a single isobestic point could be easily identified during the spectrophotometric analysis only at DNA/AO molecular ratios above 5.0). The measurement of an association constant or 'affinity' for the AO–DNA system under such conditions was assessed by both absorbance studies and fluorescence studies, and the K_{assoc} values were found to be similar (Table 3).

Data from optical titrations suggest that the AO–AO self-stacking or dimer formation is practically eliminated at high DNA/AO ratios. These data suggest that the binding process for AO to DNA at lower molecular ratios can be divided into two different processes as has been described for most of the acridine derivatives: one of high affinity (type I); and one of lower affinity (type II) [34,56]. The type I process is strong and corresponds to the intercalation of the AO into the DNA double helix at low binding ratios. Type II process is weak and is normally attributed to an external electrostatic binding at high binding ratios. The use of different fluorescence emission wavelengths allowed for the calculation of association constants for each kind of binding involved in the interaction process. Therefore, binding values determined from data obtained at $\lambda_{em}=530$ nm should be considered as relative to the intercalation or $\pi-\pi$ binding (stacking) of AO to DNA. The K_{assoc} values obtained at low AO/DNA ratios (intercalation process) were in agreement with the K_{assoc} values obtained by the spectrofluorometric method suggesting that the fluorometric determination at $\lambda_{em}=530$ nm only allows the calculation for the type I strong binding mode association constant.

At low DNA/AO molecular ratios, a decrease in the fluorescence intensity of AO was observed when interacting with DNA, primarily caused by a lowering of the fluorescence quantum yield, as occurs for many organic compounds capable of binding to nucleic acids [44]. The optical data allowed the binding constant K_{assoc} for the AO–DNA interaction to be calculated. All the data reported here show that AO has a strong binding affinity for DNA, especially at low AO concentrations. This behavior is sensitive to the concentration of the acridine chromophore as stronger binding between AO and DNA is seen at lower ratios of AO/DNA base pairs (AO concentrations <3 μmol). This is most likely due to AO being present primarily as a monomer and the absence of any significant concentration of AO dimers.

4.5. Interpretations of the results from the spectrofluorometric study on the influence of NaCl on the interaction of acridine orange with itself, with caffeine, or with dsDNA

As described above, short-range stacking interactions including hydrophobic and dispersive forces are driving these associations [14]. The protonization of AO contributes a long-range electrostatic interaction to the solvent system [33]. As illustrated in Fig. 2b, the increase of NaCl concentration to 150 mmol resulted in an increase in K_{assoc} for the dimerization of AO from 38 620 to 118 000 mol^{-1} at AO concentrations ranging from 0.5 to 5.0 μM. This is attributed to the stabilization of the AO–AO dimer by decreasing the contribution of water molecules to the solvation of the AO monomer by competing with the electrostatic charge due to the protonization of the nitrogen on AO. Thus, the higher K_{assoc} value in the presence of 150 mmol NaCl is expected to shift the equilibrium between monomeric AO and dimeric AO to favor the formation of AO dimers. Even at relatively low AO concentrations (2 μmol), physiological concentrations of NaCl caused a 23% increase in fluorescence values at $\lambda_{em}=530$ nm, indicative of an increase in dimer formation (see Table 2).

With respects to caffeine, CAF is not charged at neutral pH and therefore, K_{assoc} between AO and CAF was not expected to be sensitive to changes in ionic strength as is AO–AO self-association. The slight, but significant decrease in K_{assoc} for the AO–CAF complex from 258 to 169 mol^{-1} [14] with an increase in ionic strength, indicates that perhaps there is an ionic component in stacking interactions between AO and CAF and that in the complex, the CAF molecule may take on some negative charge. If the CAF molecule was positively charged the opposite relationship

between K_{assoc} and ionic strength would be expected. Alternatively, one could argue on thermodynamic grounds that the driving force for the formation of the AO–CAF complex is the AO molecule, and the reduction in energy gained by the formation of a complex. The AO–CAF system therefore represents a multi-equilibria system in which, among two control parameters, one (K_{assoc} for AO–AO) is positively affected by ionic strength, while the second (K_{assoc} for AO–CAF) is negatively affected by ionic strength as was suggested by Kapuscinski and Kimmel [14]. The combined fluorescence of the AO–AO dimer and the AO–CAF complex in equilibrium with monomeric AO, is reflected in the increase in fluorescence values seen for the AO–CAF system over that of AO alone.

The solution containing AO and DNA gave a fluorescence value almost double that of AO alone reflecting the high degree to which AO intercalated into the DNA. The addition of 150 mmol of NaCl to a solution containing the AO and DNA caused a 20% reduction in the fluorescence of the solution. In solutions containing NaCl, an increase in the ionic strength causes DNA to lose some of its ability to form electrostatic bonds with AO [57]. At a molecular ratio of 1000:1 (2 mmol DNA/2 μmol AO), this should have little if any effect on the fluorescence intensity of the AO–DNA complex. The addition of NaCl causes a shift in the amount of free AO monomer available for intercalation into DNA by increasing the concentration of AO–AO dimer. This increase in the formation of AO–AO dimers would cause a decrease in fluorescence intensity by reducing the concentration of AO–DNA complexes formed from 2 to 1 for every dimer formed.

4.6. Competitive interactions of CAF, DNA, and AO in the presence and absence of physiological concentrations of NaCl based on the interpretation of the fluorescence intensity at $\lambda_{em}=530$ nm

Because the AO–AO dimer has a relatively high K_{assoc}, it competes favorably for monomeric AO vs. binding to dsDNA or CAF. At low AO concentrations (<5 μmol), the presence of dimeric AO is negligible, yet both dsDNA and/or CAF still have to compete against the AO self-association constant for dimerization in order to form a complex. Charge modification of monomeric AO by the addition of NaCl at low AO concentrations, facilitates AO–AO self-association and enhances the K_{assoc} value three-fold, by modifying the electrostatic charge site and the electro-repulsive forces between AO molecules. Therefore, at AO concentrations <5 μmol, the presence of physiological concentrations of NaCl causes the K_{assoc} for the formation of the AO–AO dimer to be the primary force for the tying up of AO monomers into dimeric forms, thus lessening the chance that a AO monomer will interact with DNA or CAF. In support of this conclusion, Table 2 shows a significant increase in the concentration of AO–AO dimers and therefore, a decrease in AO monomers as evidenced by an increase in fluorescence at $\lambda_{em}=530$ nm when NaCl is added to AO.

Caffeine is supposedly not charged at neutral pH and therefore, K_{assoc} between AO and CAF was not expected to be sensitive to changes in ionic strength as is AO–AO self-association. However, the slight but significant decrease in K_{assoc} for the AO–CAF complex from 258 to 169 mol^{-1}, with an increase in ionic strength indicates that perhaps there is an ionic component in the interaction between AO and CAF and that in the AO–CAF complex, the CAF molecule may have a modest negative charge. The AO–CAF system therefore represents a multi-equilibria system in which, among two control parameters, one (K_{assoc} for AO–AO dimerization) is positively affected by ionic strength, while the second (K_{assoc} for AO–CAF) is negatively affected by ionic strength as was suggested by Kapuscinski and Kimmel [14]. This opposite effect of 125 mmol NaCl on AO and CAF at near neutral pH tended to cancel each other out, resulting in no significant change in the fluorescence of the AO–CAF system when NaCl is added (see Table 2).

In the case of dsDNA, an increase in ionic strength of the system as with the addition of NaCl, may reduce its ability to form electrostatic bonds to AO [59]. This may affect the intensity of fluorescence for AO when intercalated into DNA and/or increase the concentration of AO–AO dimer causing an increase in fluorescence

intensity at $\lambda_{em}=530$ nm. However, the addition of NaCl to the system should have little if any effect on the ability of DNA to form intercalation complexes with monomers of AO at an AO concentration of 2 μmol. Results from Table 2 show that the addition of NaCl to the AO–DNA system causes a significant decrease in fluorescence. This decrease is due to an increase in AO–AO dimerization with a lower intensity of fluorescence than when AO is fully intercalated into dsDNA. Contributing to this decrease in fluorescence is the overall decrease in the amount of monomeric AO and therefore, a corresponding reduction in the amount of AO available for dimerization and intercalation into the DNA.

In a solution containing all three reactants, the equilibrium in the AO–CAF–DNA system is controlled by four parameters, i.e. K_{AO-AO}, K_{AO-CAF}, $K_{AO-DNA\ (i)}$ and $K_{AO-DNA\ (e)}$, which represent the (at AO > 5 μmol) association constants for AO–AO, AO–CAF, AO–DNA (intercalation), and AO–DNA (electrostatic), respectfully. The K_{eq} for the system would be:

$$K_{eq}=K_{AO—AO}+K_{AO—CAF}+K_{AO—DNA(i)}+K_{AO—DNA(e)}$$

At any given concentration of AO, at constant temperature, pH, and pressure, K_{eq} is a constant. Changes in the K_{assoc} values for AO–AO, AO–CAF, or AO–$DNA_{(i/e)}$ will not affect the overall K_{eq} of the system, but will instead affect the K_{assoc} values between the other reactants. Results from the interaction of all three reactants in the absence and presence of NaCl, support this concept. However, the K_{assoc} values for each reactant reflects the molecular interaction with the AO monomer and assumes that the concentration of AO in solution is entirely in monomeric form. The results indicate that at AO concentrations < 5 μmol, this is a reasonable assumption and interpretation of fluorometric measurement of interactions between AO, dsDNA, CAF, and NaCl are relatively simple. At AO concentrations > 5 μmol, the assumption that AO is exclusively in monomeric form is invalid. Even at AO concentrations > 5 μmol, one can still interpret the spectrofluorometric data at $\lambda_{em}=530$ nm as discussed next.

The model presented in Fig. 11 illustrates the molecular populations of AO at 2 and 20 μmol. At a concentration of 2 μmol, AO is almost exclusively in monomeric form whereas at a concentration of 20 μmol, there exists a dynamic equilibrium between the monomeric and multimeric forms. The monomer form of AO reacts with CAF to form an AO–CAF complex (also shown in Fig. 11) and only the monomeric form of AO can intercalate into dsDNA. The availability of monomeric AO is critical to its intercalation into dsDNA and/or its complexation with CAF. Conditions that affect the equilibrium between the multimeric and monomeric forms of AO, such as NaCl, effect the overall concentration and availability of monomeric AO. Table 2 shows that the addition of CAF to the AO–DNA system causes a significant decrease in fluorescence with no significant decrease upon the addition of NaCl. This suggests that the relatively high concentration of CAF (5 mmol) is able to reduce the amount of AO intercalated into DNA through competitive complexation of monomeric AO, based on mass action. The addition of CAF to the AO–DNA–NaCl system causes no significant change in fluorescence, as would be expected due to the non-charged state of CAF.

Studies on the effects of 150 mmol NaCl and 2 mmol dsDNA on the interaction of 20 μmol AO to increasing concentration of CAF are depicted in Fig. 9. The results from this experiment on the effect of NaCl concentration can be explained by the stabilization of the AO–AO dimer, and the formation of the AO–CAF complex as evidenced by the uniform decrease in fluorescence values. The K_{assoc} value for AO–CAF complex in the presence of 150 mmol NaCl drops from 254 to 169 mol^{-1} contributing to the drop in fluorescence seen in both Figs. 8 and 9 for the AO–CAF–NaCl system. Also contributing to this drop in fluorescence is the stabilization of the AO–AO dimer by neutralization of charge-repulsion as mentioned earlier. The addition of dsDNA to the system containing AO, CAF and NaCl, shows a further decrease in the fluorescence values at $\lambda_{em}=530$ nm, suggesting the additional interaction of the AO monomer to the phosphate backbone of the DNA contributing to a reduction in the availability

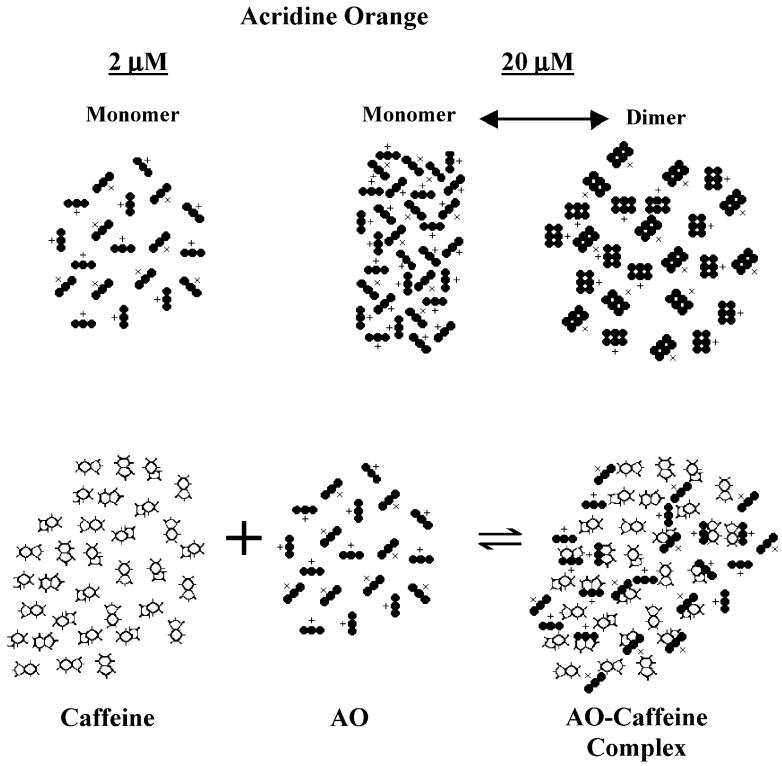

Fig. 11. Schematic showing the relative population of AO monomers and dimers at concentrations of 2 (upper left) and 20 μmol (upper right), and the binding of AO monomers to individual molecules of caffeine (lower right).

of the AO monomer for interaction with itself (dimerization) and CAF.

The results of experiments that increased concentration of AO in the presence of CAF, dsDNA, and/or NaCl, as shown in Fig. 8, reveal that the interaction of CAF with increasing AO concentration follows the law of mass action in that fluorescence increases proportional to the increase in AO concentration. The addition of 20 μmol dsDNA to the AO–CAF system causes a significant reduction in fluorescence response. This is attributed to the electrostatic bonding of AO to the DNA backbone and therefore, a reduction in available AO monomers for AO–AO dimerization and for complexation with CAF thus resulting in the lowering of the fluorescence intensity. The addition of NaCl to this system slightly increases the amount of fluorescence along the series of increasing AO concentrations and can be attributed to charge neutralization of the phosphate group on the DNA backbone, freeing up monomeric AO as well as the ability of NaCl to stabilize AO–AO dimers. The charge neutralization of the phosphate backbone on DNA also results in a shift to more monomeric AO, contributing to the formation of AO–CAF complexes and/or AO–DNA intercalation resulting in a higher fluorescent intensity.

Fig. 10 compares the effect of increasing concentrations of dsDNA on the interactions of AO, CAF, and/or NaCl by observing fluorescence intensity at $\lambda_{em} = 530$ nm. Initial additions of dsDNA to 20 μmol AO results in a steep drop in fluorescence attributed to a combination of factors; reduction in monomer AO by both intercalation into dsDNA and electrostatic bonding to dsDNA, plus a shift from dimeric AO that fluoresces at $\lambda_{em} = 530$ nm to monomeric AO, which does not fluoresce. The addition of CAF slightly increases

the fluorescence at $\lambda_{em}=530$ nm as it competes for available monomer AO. This increase in fluorescence is attributable to the formation of AO–CAF complexes. The addition of NaCl to the AO–CAF–DNA system allows for the charge neutralization of the phosphate backbone of the DNA molecule, and the subsequent increase in the availability of monomer AO to form fluorescent complexes with CAF and dsDNA, thereby causing an increase in the overall fluorescence values. This supports the concept that the initial drop in fluorescence values was due primarily to the electrostatic binding of monomeric AO to the phosphate backbone of DNA that does not fluoresce at $\lambda_{em}=$ 530 nm.

4.7. Final comments on the interactions between acridine orange, caffeine and dsDNA

Data in Table 3 summarize the K_{assoc} for the various interactions between AO, CAF and DNA from this and past reports in the literature. These data and the other experimental findings can be explained as follows:

When the DNA intercalator AO is mixed with CAF, a multiple equilibrium system is formed in which several types of interactions exist: (a) CAF, in solution at high concentrations, undergoes self-association to form indefinite-sized aggregates (multimers) in equilibrium with monomeric CAF [58–60]; (b) most DNA intercalators, including AO, self-associate in aqueous solutions and their self-interaction at low concentrations (<50 μmol) is limited [33,34,61]; and (c) spectroscopic studies [9,11,14] indicate that AO–CAF complex formation is in equilibrium with CAF–CAF multimers, monomers of AO and CAF, and AO–AO dimers.

The concentration of AO used in the various reactions is critical to predicting fluorescence intensity and values for K_{assoc} between reactants. The reason is that when AO reaches a critical concentration between 4 and 5 μmol, it self-associates to form multimers as characterized by a much higher fluorescence at $\lambda_{em}=530$ nm. One possible explanation is that when the concentration of monomeric AO reaches a critical thermodynamic point (concentration), there is a shift in the AO/AO–AO equilibrium from primarily monomer, to monomer plus dimer and possibly unstacked dimer aggregates. This critical concentration for the increase in the fluorescence of AO is shifted to an even lower concentration (i.e. 3.5 μmol) in the presence of DNA. This may be explained by the presence of the large DNA structure that may provide a stable platform for AO dimer formation by acting as a nidation or nucleation site, thus effectively lowering the energy of AO–AO dimer formation. Because the AO–AO dimer has a relatively high K_{assoc} it competes favorably for monomeric AO vs. binding to DNA or to CAF. At low AO concentrations (<5 μmol), the presence of dimeric AO is negligible yet both DNA and/or CAF must still compete with the thermodynamic driving force for AO dimerization, in order to form a complex. Charge modification of monomeric AO by the addition of NaCl facilitates AO–AO self-association and enhances the K_{assoc} value threefold by modifying the electrostatic charge site and the electro-repulsive forces between AO molecules. Therefore, at AO concentrations <5 μmol, the presence of physiological concentrations of NaCl causes the K_{assoc} for the formation of the AO–AO dimer to be the primary force for tying up of AO monomers and thus inhibiting their interaction with DNA or CAF.

These findings proved useful in explaining the fluorescence intensity at $\lambda_{em}=530$ nm of mixtures of CAF, DNA and AO.

Acknowledgments

The authors thank Dr W.E. Hardman and Mr Jesse Munoz for invaluable help and comments throughout all of our work, and Dr G.I. Henderson for kindly allowing us the use of the spectrophotometer. Additional thanks to Drs M. MacLeod and H.R. Rawls for their helpful and informative discussions, and to Dr G. Adrian and Dr P. Jagadeeswaran for the reading and comments on earlier drafts of this report. This work was supported in part by a grant from the National Institute of Dental Research, Dentist Scientist Program (DE00152).

References

[1] E.C. Miller, J.A. Miller, Mechanisms of chemical carcinogenesis, Cancer 47 (1981) 1055–1064.

[2] E.C. Miller, J.A. Miller, Searches for ultimate chemical carcinogens and their reactions with cellular macromolecules, Cancer 47 (1981) 2327–2345.
[3] M.C. MacLeod, W.G. Qing, K.L. Powell, A. Daylong, F.E. Evans, Reaction of non-toxic, potentially chemopreventive purinethiols with a direct-acting, electrophilic carcinogen, benzo[*a*]pyrene-7,8-diol 9,10-epoxide, Chem. Res. Toxicol. 6 (1993) 159–167.
[4] R. Dashwood, D. Guo, Inhibition of 2-amino-3-methylimidazo[4,5-f]quinoline (IQ)-DNA binding by chlorophyllin: studies of enzyme inhibition and molecular complex formation, Carcinogenesis 13 (1992) 1121–1126.
[5] R. Dashwood, D. Guo, Antimutagenic potency of chlorophyllin in the Salmonella assay and its correlation with binding constants of mutagen–inhibitor complexes, Environ. Mol. Mutagen. 22 (1993) 164–171.
[6] P.E. Hartman, D.M. Shankel, Antimutagens and anticarcinogens: a survey of putative interceptor molecules [published erratum appears in Environ. Mol. Mutagen. 16 (2) (1990) 136], Environ. Mol. Mutagen. 15 (1990) 145–182.
[7] C. Ramel, U.K. Alekperov, B.N. Ames, T. Kada, L.W. Wattenberg, International Commission for Protection Against Environmental Mutagens and Carcinogens. ICPEMC publication no. 12. Inhibitors of mutagenesis and their relevance to carcinogenesis. Report by ICPEMC Expert Group on Antimutagens and Desmutagens, Mutat. Res. 168 (1986) 47–65.
[8] N. Tachino, D. Guo, W.M. Dashwood, S. Yamane, R. Larsen, R. Dashwood, Mechanisms of the in vitro antimutagenic action of chlorophyllin against benzo[*a*]pyrene: studies of enzyme inhibition, molecular complex formation and degradation of the ultimate carcinogen, Mutat. Res. 308 (1994) 191–203.
[9] R.W. Larsen, R. Jasuja, R.K. Hetzler, P.T. Muraoka, V.G. Andrada, D.M. Jameson, Spectroscopic and molecular modeling studies of caffeine complexes with DNA intercalators, Biophys. J. 70 (1996) 443–452.
[10] F. Traganos, B. Kaminska-Eddy, Z. Darzynkiewicz, Caffeine reverses the cytotoxic and cell kinetic effects of novantrone (mitoxantrone), Cell Prolif. 24 (1991) 305–319.
[11] F. Traganos, J. Kapuscinski, Z. Darzynkiewicz, Caffeine modulates the effects of DNA-intercalating drugs in vitro: a flow cytometric and spectrophotometric analysis of caffeine interaction with novantrone, doxorubicin, ellipticine, and the doxorubicin analogue AD198, Cancer Res. 51 (1991) 3682–3689.
[12] F. Traganos, J. Kapuscinski, J. Gong, B. Ardelt, R.J. Darzynkiewicz, Z. Darzynkiewicz, Caffeine prevents apoptosis and cell cycle effects induced by camptothecin or topotecan in HL-60 cells, Cancer Res. 53 (1993) 4613–4618.
[13] M.C. MacLeod, K.L. Mann, G. Thai, C.J. Conti, J.J. Reiners, Inhibition by 2,6-dithiopurine and thiopurinol of binding of a benzo(a)pyrene diol epoxide to DNA in mouse epidermis and of the initiation phase of two-stage tumorigenesis, Cancer Res. 51 (1991) 4859–4864.
[14] J. Kapuscinski, M. Kimmel, Thermodynamical model of mixed aggregation of intercalators with caffeine in aqueous solution, Biophys. Chem. 46 (1993) 153–163.
[15] P.J.A. McKeown, A.R. Ubbelohde, I. Woodward, Thermal expansion of *p*-nitroaniline and *p*-dinitrobenzene, Acta Cryst. 4 (1951) 391–395.
[16] J. Booth, E. Boyland, The reaction of the carcinogenic dibenzacarbazoles and dibenzacridines with purines and nucleic acid, Biochem. Biophys. Acta 12 (1953) 75–87.
[17] M. Shoyab, Caffeine inhibits the binding of dimethylbenz(a)anthracene to murine epidermal cells DNA in culture, Arch. Biochem. Biophys. 196 (1979) 307–310.
[18] T.T. Harding, S.C. Wallwork, The structure of molecular compounds exhibiting polarization bonding. I. General introduction and the crystal structure of phenoquinone, Acta Cryst. 6 (1953) 791–796.
[19] T.T. Harding, S.C. Wallwork, The structure of molecular compounds exhibiting polarization bonding. II. The crystal structure of the chloranil–hexamethylbenzene complex, Acta Cryst. 8 (1955) 787–794.
[20] S.C. Wallwork, Molecular complexes exhibiting polarization bonding. III. A structural survey of some aromatic complexes, J. Chem. Soc. (1961) 494–499.
[21] A.M. Liquori, B. DeLerma, F. Ascoli, M. Transciatti, Interaction between DNA and polycyclic aromatic hydrocarbons, J. Mol. Biol. 5 (1962) 521–526.
[22] J. Miller, Carcinogenesis by chemicals: an overview—G.H.A. Clowes memorial lecture, Cancer Res. 30 (1970) 559–576.
[23] E. Huberman, L. Sachs, H. Yamasaki, DNA binding and its relationship to carcinogenesis by different polycyclic hydrocarbons, Int. J. Cancer 19 (1976) 122–127.
[24] F. DeSantis, E. Giglio, A.M. Liquori, Crystal structure of 1,3,7,9-tetramethyluric acid and the molecular packing in hydromethyl purine crystals, Nature 188 (1960) 46–48.
[25] F. DeSantis, E. Giglio, A.M. Liquori, A. Pipamonti, Molecular geometry of a 1:1 crystalline complex between 1,3,7,9-tetramethyluric acid and pyrene, Nature 191 (1961) 900–901.
[26] B.L. Van Duuren, Fluorescence of 1,3,7,9-tetramethyluric acid complexes of aromatic hydrocarbons, J. Phys. Chem. 68 (1964) 2544–2553.
[27] B. Pullman, Electronic aspects of the interactions between the carcinogens and possible cellular sites of their activity, J. Cell. Comp. Physiol. 64 (suppl. 1) (1964) 91–109.
[28] R. Ganapathi, D. Grabowski, H. Schmidt, A. Yen, G. Iliakis, Modulation of adriamycin and *N*-trifluoroacetyladriamycin-14-valerate-induced effects on cell cycle traverse and cytotoxicity in P388 mouse leukemia cells by caffeine and the calmodulin inhibitor trifluoperazine, Cancer Res. 46 (1986) 5553–5557.
[29] G. Iliakis, M. Nusse, R. Ganapathi, J. Egner, A. Yen, Differential reduction by caffeine of adriamycin-induced

cell killing and cell cycle delays in Chinese hamster V79 cells, Int. J. Rad. Oncol. Biol. Phys. 12 (1986) 1987–1995.

[30] K. Rothwell, Dose-related inhibition of chemical carcinogenesis in mouse skin by caffeine, Nature 252 (1974) 69–70.

[31] M.B. Lyles, Filters for polynuclear aromatic hydrocarbon containing smoke, United States Patent 4,517,995, 1985.

[32] E. Boyland, B. Green, The interaction of polycyclic hydrocarbons and purines, Br. J. Cancer 16 (1962) 347–360.

[33] B.H. Robinson, A. Loffler, G. Schwarz, Thermodynamic behavior of acridine orange in solution. Model system for studying stacking and charge effects on self-aggregation, J. Chem. Soc. Faraday Trans. 69 (1) (1973) 56–69.

[34] J. Kapuscinski, Z. Darzynkiewicz, Interactions of acridine orange with double stranded nucleic acids. Spectral and affinity studies, J. Biomol. Struct. Dyn. 5 (1987) 127–143.

[35] J. Kapuscinski, Z. Darzynkiewicz, Spectral properties of fluorochromes used in flow cytometry, Methods Cell Biol. 33 (1990) 655–669.

[36] V. von Tscharner, G. Schwarz, Complex formation of acridine orange with single-stranded polyriboadenylic acid and 5′-AMP: co-operative binding and intercalation between bases, Biophys. Struct. Mech. 5 (1979) 75–90.

[37] H.A. Benesi, J.H. Hildebrand, A spectrophotometric investigation of the interaction of iodine with aromatic hydrocarbons, J. Chem. Soc. 71 (1949) 2703–2707.

[38] K.A. Connors, Binding Constants: The Measurement of Binding Complex Stability, John Wiley and Sons, New York, 1987, pp. 75–149.

[39] R. Zaini, A.C. Orcitt, B.R. Arnold, Determination of equilibrium constants for weakly bound charge–transfer complexes, Photochem. Photobiol. 69 (1999) 443–447.

[40] R.P. Haugland, Spectra of fluorescent dyes used in flow cytometry, Methods Cell Biol. B 42 (1994) 641–663.

[41] Z. Darzynkiewicz, Simultaneous analysis of cellular RNA and DNA content, Meth. Cell Biol. 41 (1994) 401–420.

[42] J. Kapuscinski, Z. Darzynkiewicz, Denaturation of nucleic acids induced by intercalating agents. Biochemical and biophysical properties of acridine orange–DNA complexes, J. Biomol. Struct. Dyn. 1 (1984) 1485–1499.

[43] Z. Darzynkiewicz, Differential staining of DNA and RNA in intact cells and isolated cell nuclei with acridine orange, Methods Cell Biol. 33 (1990) 285–298.

[44] J. Kapuscinski, Interactions of nucleic acids with fluorescent dyes: spectral properties of condensed complexes, J. Histochem. Cytochem. 38 (1990) 1323–1329.

[45] V. Zanker, The proof of definite reversible association of acridine orange by absorbance and fluorescence measurements in aqueous solution, Z. Physik. Chem. 199 (1952) 225–258.

[46] N.G. Bakhshiev, The internal field and the position of the electronic absorption and emission bands of polyatomic organic molecules in solution, Optika i Spectroskopiya 7 (1959) 52–61.

[47] N.G. Bakhshiev, Dielectric effects and properties of electronic spectra of multiatomic organic molecules in solution, Izvest. Akad. Nauk S.S.S.R. Ser. Fiz. 24 (1960) 587–590.

[48] N.G. Bakhshiev, Universal intermolecular interactions and their effects on the position and electronic spectra of molecules in two-component solutions, Opt. Spectrosc. 10 (1961) 379–384.

[49] C.P. Selby, A. Sancar, Molecular mechanism of DNA repair inhibition by caffeine, Proc. Natl. Acad. Sci. USA 87 (1990) 3522–3525.

[50] S. Arimoto, S. Fukuoka, C. Itome, H. Nakano, H. Rai, H. Hayatsu, Binding of polycyclic planar mutagens to chlorophyllin resulting in inhibition of the mutagenic activity, Mutat. Res. 287 (1993) 293–305.

[51] D.R. Langley, T.W. Doyle, D.L. Beveridge, The dynemicin–DNA intercalation complex: a model based on DNA affinity cleavage and molecular dynamics simulation, J. Am. Chem. Soc. 113 (1991) 4395–4403.

[52] Z. Darzynkiewicz, F. Traganos, J. Kapuscinski, M.R. Melamed, Denaturation and condensation of DNA in situ induced by acridine orange in relation to chromatin changes during growth and differentiation of Friend erythroleukemia cells, Cytometry 6 (1985) 195–207.

[53] Z. Darzynkiewicz, F. Traganos, Unstainable DNA in cell nuclei. Comparison of ten different fluorochromes, Anal. Quant. Cyto. Hist. 10 (1988) 462–466.

[54] J. Kapuscinski, DAPI: a DNA-specific fluorescent probe, Biotechnol. Histochem. 70 (1995) 220–233.

[55] I. Haq, J.E. Ladbury, B.Z. Chowdhry, T.C. Jenkins, J.B. Chaires, Specific binding of Hoechst 33258 to the d(CGCAAATTTGCG)$_2$ duplex: calorimetric and spectroscopic studies, J. Mol. Biol. 271 (1997) 244–257.

[56] E. Gimenez-Arnau, S. Missailidis, M.F. Stevens, Antitumour polycyclic acridines. Part 4. Physico-chemical studies on the interactions between DNA and novel tetracyclic acridine derivatives, Anti-Cancer Drug Des. 13 (1998) 431–451.

[57] J. Delic, J. Coppey, H. Magdelenat, M. Coppey-Moisan, Impossibility of acridine orange intercalation in nuclear DNA of the living cell, Exp. Cell Res. 194 (1991) 147–153.

[58] L.H. Tang, D.R. Powell, B.M. Escott, E.T. Adams, Analysis of various indefinite self-associations, Biophys. Chem. 7 (1977) 121–139.

[59] H. Fritzsche, H. Lang, H. Sprinz, W. Pohle, On the interaction of caffeine with nucleic acids. IV. Studies of

the caffeine–DNA interaction by infrared and ultraviolet linear dichroism, proton and deuteron nuclear magnetic resonance, Biophys. Chem. 11 (1980) 121–131.
[60] H. Fritzsche, I. Petri, H. Schutz, K. Weller, P. Sedmera, H. Lang, On the interaction of caffeine with nucleic acids. III. ^{1}H NMR studies of caffeine–5′-adenosine monophosphate and caffeine–poly(riboadenylate) interactions, Biophys. Chem. 11 (1980) 109–119.
[61] J. Kapuscinski, Z. Darzynkiewicz, Interactions of antitumor agents ametantrone and mitoxantrone (novatrone) with double-stranded DNA, Biochem. Pharm. 34 (1985) 4203–4213.